



STANDARD ARTICLE

Extracellular vesicular microRNAs as potential biomarker for early detection of doxorubicin-induced cardiotoxicity

Amelie Beaumier¹ | Sally R. Robinson¹ | Nicholas Robinson² | Katherine E. Lopez¹ | Dawn M. Meola¹ | Lisa G. Barber¹ | Barret J. Bulmer³ | Jerome Calvalido³ | John E. Rush¹  | Ashish Yeri⁴ | Saumya Das⁴ | Vicky K. Yang¹ 

¹Department of Clinical Sciences, Cummings School of Veterinary Medicine at Tufts University, North Grafton, Massachusetts

²Department of Biomedical Sciences, Cummings School of Veterinary Medicine at Tufts University, North Grafton, Massachusetts

³Tufts Veterinary Emergency Treatment & Specialties, Walpole, Massachusetts

⁴Cardiovascular Research Center, Massachusetts General Hospital, Boston, Massachusetts

Correspondence

Vicky K. Yang, Department of Clinical Sciences, Cummings School of Veterinary Medicine at Tufts University, 200 Westboro Road, North Grafton MA 01536.
 Email: vicky.yang@tufts.edu

Funding information

American Heart Association; Barkley Fund; National Institutes of Health (NIH), Grant/Award Number: RO1 HL122547; Shipley Foundation; Tufts Companion Animal Health Fund

Abstract

Background: Long-term use of doxorubicin (DOX) is limited by cumulative dose-dependent cardiotoxicity.

Objectives: Identify plasma extracellular vesicle (EV)-associated microRNAs (miRNAs) as a biomarker for cardiotoxicity in dogs by correlating changes with cardiac troponin I (cTnI) concentrations and, echocardiographic and histologic findings.

Animals: Prospective study of 9 client-owned dogs diagnosed with sarcoma and receiving DOX single-agent chemotherapy (total of 5 DOX treatments). Dogs with clinically relevant metastatic disease, preexisting heart disease, or breeds predisposed to cardiomyopathy were excluded.

Methods: Serum concentration of cTnI was monitored before each treatment and 1 month after the treatment completion. Echocardiography was performed before treatments 1, 3, 5, and 1 month after completion. The EV-miRNA was isolated and sequenced before treatments 1 and 3, and 1 month after completion.

Results: Linear mixed model analysis for repeated measurements was used to evaluate the effect of DOX. The miR-107 ($P = .03$) and miR-146a ($P = .02$) were significantly downregulated whereas miR-502 ($P = .02$) was upregulated. Changes in miR-502 were significant before administration of the third chemotherapeutic dose. When stratifying miRNA expression for change in left ventricular ejection fraction, upregulation of miR-181d was noted ($P = .01$). Serum concentration of cTnI changed significantly but only 1 month after treatment completion, and concentrations correlated with left ventricular ejection fraction and left ventricular internal dimension in diastole.

Abbreviations: cTnI, cardiac troponin I; DOX, doxorubicin; E', peak myocardial velocity in early diastole; ECG, electrocardiography; EV, extracellular vesicle; EV-miRNA, extracellular vesicle-associated miRNA; FAC, fractional area change; FS, fractional shortening; IVCT, isovolumic contraction time; IVRT, isovolumic relaxation time; LA:Ao, left atrium to aorta ratio; LVEF, left ventricular ejection fraction; LVIDdN, left ventricular end-diastolic internal diameter normalized to body weight; LVIDsN, left ventricular end-systolic internal diameter normalized to body weight; miRNAs, microRNAs; S', peak myocardial velocity in systole.

This is an open access article under the terms of the Creative Commons Attribution-NonCommercial License, which permits use, distribution and reproduction in any medium, provided the original work is properly cited and is not used for commercial purposes.

© 2020 The Authors. *Journal of Veterinary Internal Medicine* published by Wiley Periodicals, Inc. on behalf of the American College of Veterinary Internal Medicine.

Conclusion and Clinical Significance: Downregulation of miR-502 was detected before significant changes in cTnI concentrations or echocardiographic parameters. Further validation using a larger sample size will be required.

KEYWORDS

chemotherapy, echocardiogram, ejection fraction, hemangiosarcoma, troponin

1 | INTRODUCTION

Doxorubicin (DOX) is an anthracycline chemotherapeutic agent that can be used to treat a wide range of hematologic and solid tumors.¹ Its long-term use is limited by cumulative dose-dependent cardiotoxicity that generally is irreversible.² Anthracycline cumulative dose remains the most important risk factor for development of cardiotoxicity in both human and veterinary cancer patients.³

Currently, no standardized cardiac monitoring protocol is available for veterinary patients receiving anthracycline treatment. In contrast, standard protocols in human medicine include serial assessment of the left ventricular ejection fraction (LVEF) using noninvasive cardiac imaging,⁴ including radionuclide angiography, transthoracic echocardiography, and cardiac magnetic resonance imaging.⁵ A decrease in LVEF of $\geq 5\%$ to $< 55\%$ with signs of congestive heart failure or a decrease in LVEF of $\geq 10\%$ to $< 55\%$ without clinical signs may prompt suspension of treatment.³ However, decreases in LVEF often are detected only after functional impairment has occurred, precluding any chance of reversing cardiac injury.

Cardiac troponin I (cTnI) is commonly utilized as a biomarker for detecting cardiomyocyte injury, as it is highly specific and sensitive.^{6,7} However, studies in humans failed to identify a clear relationship between cTnI and myocardial dysfunction secondary to DOX treatment.^{4,8,9} In veterinary medicine, serum cTnI concentration was found to increase after serial treatment with DOX,^{7,10-12} but optimal timing for measuring serum cTnI concentration remains controversial. Furthermore, cTnI as a biomarker has several limitations including poor assay stability and increased concentrations that generally occur only after recent damage to cardiomyocytes.¹³

MicroRNAs (miRNAs) are small (22-25 nucleotides), noncoding RNAs that can inhibit gene expression by complementary binding to mRNA, thereby inhibiting protein translation or promoting degradation.¹⁴ As a result, miRNAs can affect various aspects of cell metabolism, influencing processes such as differentiation, regeneration, and apoptosis, and therefore are implicated in disease pathogenesis, making them attractive as indicators of disease state. In addition, miRNAs are released by cells into biofluids,¹⁵ where they are relatively stable and can withstand prolonged periods of storage even at room temperature.^{16,17} Their stability is in part provided by membrane-bound nanoscale entities called extracellular vesicles (EVs). Extracellular vesicles (ie, exosomes and microvesicles), increasingly have been recognized for their contribution to cell signaling, playing a role in cellular processes contributing to fibrosis, apoptosis, autophagy, and signaling pathways.^{18,19} Extracellular vesicles can contain mRNA, noncoding

RNA such as miRNA, lipids, and proteins, and their contents are highly regulated by the cell of origin, depending on the physiologic and pathologic molecular signals at work during the time of EV production. Pathologic signaling through EVs has been identified in propagation of neurologic diseases and cancer.²⁰ Extracellular vesicle-associated miRNAs (EV-miRNA) carry signals specific to the state of the cells, including signals that may indicate toxic injury. The content of miRNAs within EVs may serve as a predictive biomarker for cancer treatments.²¹

To our knowledge, changes in EV-miRNA in dogs receiving DOX treatment have not been investigated. Our aims were to identify plasma EV-miRNA expression changes in dogs receiving DOX and to correlate these changes with serum cTnI concentration, as well as echocardiographic, electrocardiographic, and histologic findings.

2 | MATERIALS AND METHODS

2.1 | Study population

This prospective study was approved by the Cummings School of Veterinary Medicine at Tufts University Institutional Animal Use and Care Committee. Client-owned dogs were included in the study if they previously had been diagnosed with sarcoma and were scheduled to begin a DOX single agent chemotherapeutic protocol at the Cummings School of Veterinary Medicine Foster Hospital for Small Animal or at Tufts Veterinary Emergency Services. The cancer type was confirmed either by cytologic or histologic evaluation. The chemotherapy protocol included 5 doses of DOX given IV 2 to 3 weeks apart, with an individual target DOX dosage of 30 mg/m² for dogs > 15 kg and 1 mg/kg for dogs < 15 kg. Dogs were still included in the study if DOX treatment was discontinued by the attending oncology and cardiology clinicians before completion of treatment because of concern for cardiotoxicity based on serum cTnI concentration, or echocardiographic or electrocardiographic findings. Exclusion criteria included breed predisposed to cardiomyopathy (eg, Doberman, Pinchers, Boxers), presence of clinically relevant metastatic disease before to the start of chemotherapy, presence of a cardiac mass, and preexisting heart disease including decreased contractile function, clinically relevant arrhythmia or mitral regurgitation, or severe pulmonary hypertension.

The following variables were evaluated: serum cTnI concentration, ECG, echocardiography, EV-miRNA expression by RNA sequencing, and cardiac histology. The timeline of the study is shown in Table 1. A CBC was performed as part of the DOX treatment standard of care.

Table 1 Timeline of examination and diagnostic testing during the study period

	DOX 1 (pre-DOX)	DOX 2	DOX 3 (during DOX)	DOX 4	DOX 5	1 mo post-DOX completion (post-DOX)	Euthanasia
Echocardiogram	×	...	×		×	×	...
ECG	×	×	×	×	×	×	...
cTnl	×	×	×	×	×	×	...
EV-miRNA	×	...	×	×	...
Complete blood count	×	×	×	×	×	×	...
Histopathology	×

2.2 | Electrocardiogram

Six-lead ECG was performed for 5 consecutive minutes before every DOX treatment as well as at the reevaluation 1 month after completion of DOX treatment. Results were analyzed by the same observer (observer 1).

2.3 | Echocardiogram

All echocardiographic examinations were performed either by a cardiology resident (observer 1) under the supervision of a board-certified cardiologist or by a board-certified cardiologist (observer 2, observer 3). All of the measurements were obtained by the same observer (observer 1). Echocardiogram (GE Vivid E9) was performed before the first, third, and fifth DOX treatments as well as 1 month after treatment completion. All examinations were performed on unsedated dogs placed in lateral recumbency. Parameters obtained from the parasternal short axis view included: fractional shortening (FS), left atrium-to-aorta ratio (LA:Ao), left ventricular end-diastolic and end-systolic internal diameters normalized for body weight (LVIDdN and LVIDsN, respectively), and fractional area change (FAC) of the left ventricle using a short axis view. From the left apical 4-chamber view, mitral inflow (E/A ratio), peak myocardial velocities during systole (S') and early diastole (E'), tissue Doppler imaging (TDI)-derived isovolumic contraction time (IVCT) and isovolumic relaxation time (IVRT), and LVEF using the Simpson's method of disc were obtained. Measurements were made on 3 consecutive cardiac cycles, and the results were averaged. The M-mode echocardiographic values were indexed for body weight.²²

2.4 | cTnl measurement

Serum cTnl concentrations were measured using an Abbott i-STAT Handheld machine using heparinized whole blood before every DOX treatment as well as 1 month after treatment completion. A serum cTnl concentration >0.08 ng/mL was considered abnormal.

2.5 | EV-miRNA isolation and sequencing

Plasma samples collected before the first and third DOX treatments and 1 month after DOX completion were evaluated and miRNA isolated by

centrifuging whole blood at 1320g for 10 minutes immediately after blood collection to remove cells and platelets. Plasma was stored at -80°C until processing. Extracellular vesicles were isolated from approximately 1.5 mL of plasma using IZON size exclusion chromatography (qEVoriginal/70 nm). Once thawed, 500 μL aliquots of plasma were individually processed through the column according to the manufacturer's instructions. Fractions 7 to 10 were collected from each 500 μL aliquot and pooled for each time point of each patient and stored at 4°C until RNA isolation. Transmission electron microscopy was used to confirm presence and visualize morphology of EVs in the isolated fractions. The CD9 protein was confirmed in the EV fractions by immunoblot (primary antibody: Bio-Rad mouse anti-human monoclonal [MCA 469], 1:500; secondary antibody: Rockland Immunochemicals Inc., anti-mouse Ig Biotin monoclonal antibody [8817-82], 1:50), and TSG101 by ELISA analysis (Canine TSG101 ELISA Kit, Mybiosource.com, MBS077995) after concentration using Amicon Ultracel 10 kDa molecular weight cutoff centrifugal filters (Merck Millipore). Lipoprotein content was measured using high-density lipoprotein (HDL) and low-density lipoprotein (LDL) ELISA kits for dogs (MyBiosource, MBS033676 [HDL], MBS2603730 [LDL]). All samples were diluted 1:10 and compared with the ELISA kit standards. Ribonucleic acid was isolated from EV fractions using the Qiagen miRNeasy Plasma/Serum kit according to the manufacturer's directions, and RNA concentrations were measured using the Agilent Bioanalyzer. The DNA libraries for sequencing were created using the QIAseq miRNA library kit (Qiagen) and validated and quantified on a Fragment Analyzer (Advanced Analytical). The libraries then were sequenced on a HiSeq 2500 sequencer (Illumina) using High Output V4 chemistry and single read 75 bases format. The raw sequence results were processed into demultiplexed files in compressed fastq format using bcl2fq (Illumina). Adaptor sequences and unique molecular identifiers were trimmed from the resulted reads using CLC Genomic Workbench 11 (Qiagen), and sequences were mapped to miRBase v22.²³ Sequence reads counts normalization and differential expression analysis were performed using DESeq2.²⁴

2.6 | Restaging during DOX treatment

Restaging tests included thoracic radiographs and abdominal ultrasound examination before the 3rd and 5th DOX treatments. If the standard restaging schedule was declined by the owner, an alternative schedule was offered, which included thoracic radiographs before to the 4th DOX treatment.

Table 2 Cardiac troponin I levels and echocardiographic values at the 6 recheck time points

	DOX 1 (pre-DOX)	DOX 2	DOX 3 (during DOX)	DOX 4	DOX 5	1 mo post DOX completion (post-DOX)	P-value
cTnI (ng/mL)	0.05 (±0.008)	0.09 (±0.035)	0.12 (±0.029)	0.13 (±0.04)	0.11 (±0.04)	0.37 (±0.29)	.04
LVIDdN_2d (mm)	3.27 (± 0.85)		3.31 (±0.79)		3.34 (±0.69)	3.78 (±0.80)	.64
LVIDsN_2d	2.25 (±0.68)		2.19 (±0.58)		2.21 (±0.57)	2.58 (±1.07)	.63
LA_2d	2.60 (± 0.56)		2.36 (±0.66)		2.69 (±0.58)	3.00 (± 0.50)	.01
LA:Ao_2d	1.33 (±0.15)		1.27 (±0.20)		1.43 (±0.20)	1.43 (±0.26)	.02
LVIDdN_MM	1.55 (±0.14)		1.49 (±0.15)		1.53 (±0.09)	1.97 (±0.79)	.04
LVIDsN_MM	0.89 (±0.17)		0.87 (±0.15)		0.86 (±0.05)	1.34 (±0.61)	.71
LA_MM	0.93 (±0.14)		0.88 (±0.13)		0.91 (±0.18)	0.90 (±0.11)	.78
LA:Ao_MM	1.20 (±0.22)		1.20 (±0.11)		1.21 (±0.25)	1.14 (±0.19)	.46
FS_2d	31.38 (±5.19)		34.20 (±5.97)		34.36 (±6.76)	27.95 (±8.53)	.21
FS_MM	38.91 (±10.82)		38.50 (±5.19)		40 (±1.78)	28.94 (±7.00)	.02
LVEF (%)	70.04 (±7.57)		72.47 (±5.52)		67.97 (±2.88)	60.67 (±11.68)	.002
EDV (mL)	1194.35 (458-3328)		1011.12 (±953.23)		1073.27 (±875.97)	1494.86 (±1448.81)	.99
ESV	137.04 (±96.36)		198.78 (±132.43)		255.27 (±221.54)	509.77 (±480.24)	.04
FAC (%)	82.12% (±8.70)		76.66 (±10.10)		74.76 (±10.29)	60.56 (±21.56)	.01
EPSS (mm)	0.47 (±0.25)		0.46 (±0.16)		0.47 (±0.13)	0.72 (±0.23)	.08
S'	0.12 (±0.05)		0.11 (±0.03)		0.11 (±0.03)	0.10 (±0.02)	.004
IVCT (ms)	32.05 (±6.76)		41.28 (±9.54)		39.31 (±10.08)	46.40 (±9.60)	.01
IVRT (ms)	59.75 (±8.00)		56.20 (±11.60)		61.23 (±7.10)	56.05 (±9.62)	.93

Note: Means with standard deviations are listed for normally distributed data whereas median and range are listed for non-normally distributed data. The linear mixed model analysis P-values are listed.

Abbreviations: 2d, two-dimensional measurements; EDV, end-diastolic volume; EPSS, E-point to septal separation; ESV, end-systolic volume; FAC, fractional area change; IVCT, isovolumic contraction time; IVRT, isovolumic relaxation time; MM, M-mode measurements.

2.7 | Histology

When possible, heart tissue of deceased patients was collected and fixed in formalin. Histologic examination of the right atrium, right ventricle, interventricular septum, and left ventricle was performed using hematoxylin and eosin, phosphotungstic acid-hematoxylin, and trichrome stains.

2.8 | Statistical analysis

Statistical analysis was performed using commercially available statistical software (SPSS Statistic 17.0, IBM, Chicago, Illinois). A linear mixed model for the analysis of repeated measurements was used to evaluate the effect of the cumulative dose of DOX over the treatment period. A P-value of <.05 was considered significant. Direct comparison among time points for individual variables except for miRNA sequencing results was performed using the Kruskal-Wallis test followed by Bonferroni posthoc correction. The DESeq2 was used for miRNA differential expression analysis. Quantitative data were assessed for normality using the Shapiro Wilk test. Means (± SD) and medians (ranges) were used as descriptive statistics for normally and non-normally distributed continuous variables,

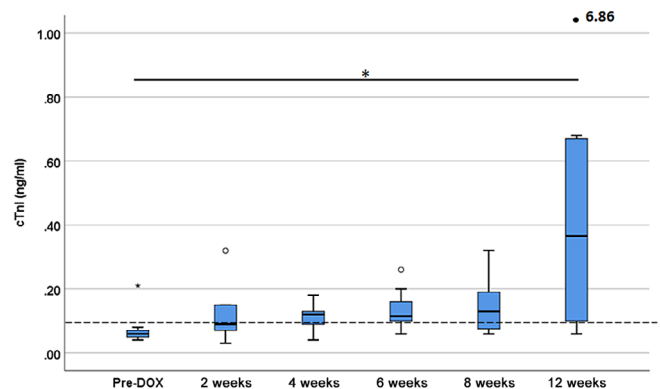


Figure 1 Linear mixed model showed significant change in cTnI values over time for the 9 dogs enrolled in the study ($P = .04$). However, pairwise comparison between time points showed only statistically significant difference ($P = .01$) between pre-DOX and post-DOX. One month after treatment completion (post-DOX), 1 patient had the highest cTnI level at 6.86 ng/mL. The dash line indicates the upper limit of normal for canine cTnI level. Large asterisk denotes significant difference. Open circles and small asterisk denote outliers

respectively. Correlation between variables was analyzed using Pearson's correlation test.

time ($P = .04$), with an increase in the mean concentration seen with additional DOX doses but direct comparison between individual time points showed a significant difference only between baseline and 1 month after completing chemotherapy ($P = .01$; Figure 1). Of the 9 dogs, only 1 had normal serum cTnI concentration throughout the treatment period. The dog that was prescribed pimobendan after the final study reevaluation had normal serum cTnI concentration before the start of chemotherapy (0.05 ng/mL) and a final concentration of 6.86 ng/mL 1 month after completing DOX treatment. A positive correlation was found between cTnI and LVIDd (0.51, $P = .002$), and negative correlations were found between cTnI and LVEF (-0.55 , $P = .001$), and between cTnI and FS (-0.39 , $P = .03$).

3.4 | Electrocardiogram

None of the dogs developed an increase in arrhythmia severity that the attending cardiologists believed warranted discontinuation of DOX treatment. Only isolated ventricular premature beats and isolated atrial premature contractions were noted. No changes in the ST segment were seen. Seven dogs had normal sinus rhythm before the start of DOX treatment and 4 of them developed some form of arrhythmia with chemotherapy.

3.5 | Complete blood count

None of the dogs developed clinically relevant anemia or thrombocytopenia during the course of the study, and blood samples did not show any notable hemolysis. Results are shown in Table S2.

3.6 | miRNA

Extracellular vesicle isolation was confirmed by positive CD9 signal on immunoblot, positive TSG101 signal measured by ELISA analysis (0.8 ng/mL of plasma), and by transmission electron microscopy (Figure 2). The IZON size exclusion chromatography yielded a total particle count of $2.5 \times 10^9 \pm 1.4 \times 10^8$ per mL of plasma, with the majority of the particles measuring between 75 and 150 μm ($1.6 \times 10^9 \pm 1.3 \times 10^8$ per mL of plasma), based on nanoparticle tracking analysis (NTA; NS300, software v3.0; Malvern). Measurement of lipoprotein showed minimal HDL (<1.5 mmol/L) and LDL (<42 ng/mL) coisolation with the EVs. High density lipoprotein-to-total particle ratio was 6.0×10^{-13} mM/mL of plasma, whereas the total protein-to-HDL ratio was 3.2×10^4 $\mu\text{g}/\text{mM}$. Low density lipoprotein-to-total particle ratio was 1.7×10^{-8} ng/mL of plasma, whereas the total protein-to-LDL ratio was 1.2×10^3 . Total protein-to-particle ratio was 1.9×10^{-8} $\mu\text{g}/\text{mL}$ of plasma. Some contribution of non-EV-associated miRNA (eg, lipoproteins) is expected because our EV isolation protocol is not designed for absolute EV purification.²⁵

The EV-miRNA analysis was performed using 8 of the 9 dogs that had hemangiosarcoma as their cancer type. The 1 dog with

leiomyosarcoma was removed from this part of the comparison to eliminate cancer type as a confounding factor for miRNA expression changes. A total of 200 miRNA sequences matched to the miRBase 22 database.²³ Of those, 3 miRNAs reached statistically significant change ($P < .05$) using both linear mixed model and DESeq2 analyses, and DESeq2 analysis was adjusted for sex and age of the patients across the 3 time points: Time 1: before starting DOX, referred to as pre-DOX; Time 2: before the 3rd DOX treatment, referred as during DOX; Time 3: 1 month after completing the last DOX treatment, referred as post-DOX (Figure 3). These miRNAs included miR-107 ($P = .03$), miR-146a ($P = .02$), and miR-502 ($P = .02$); (Figure 4). The miR-107 was significantly downregulated at post-DOX compared to

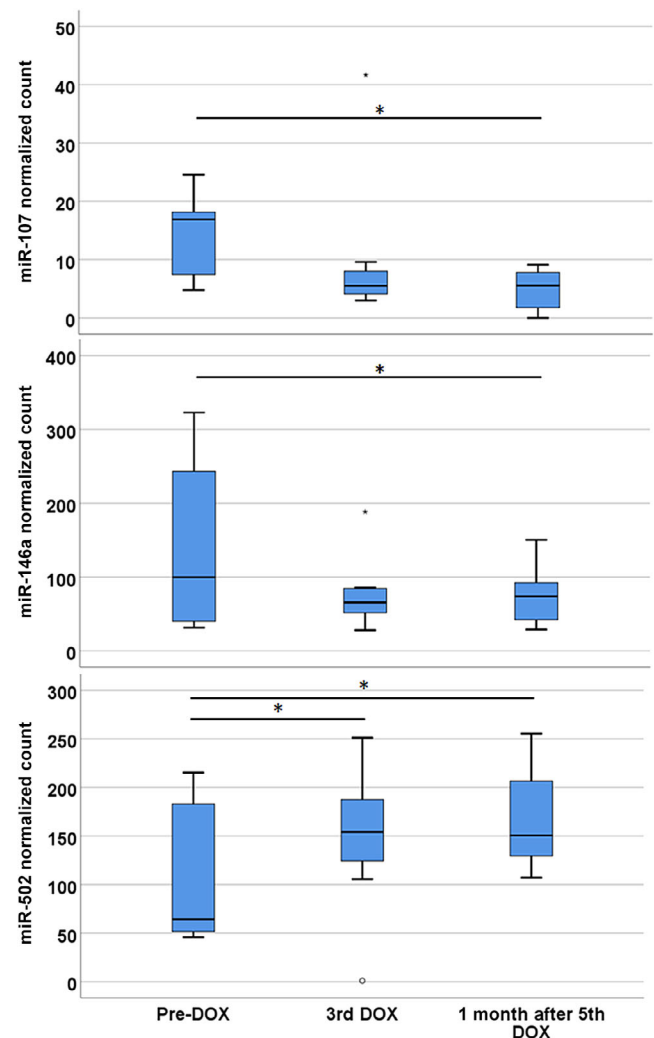


Figure 4 Box plot for the 3 miRNAs (miR-107: top, $P = .03$; miR-146a: middle, $P = .02$; miR-502: bottom, $P = .02$) that showed statistically significant changes over time using both linear mixed model analysis and DESeq2 analysis. Pairwise comparison showed that the post-DOX level of miR-107 is significantly decreased from pre-DOX level ($P = 0.04$), and similar changes were seen for miR-146a ($P = .01$). On the other hand, miR-502 levels increased significantly during DOX ($P = .01$) and post-DOX ($P = .003$). Large asterisks denote statistical significance. Open circle and small asterisks denote outliers ($n = 8$)

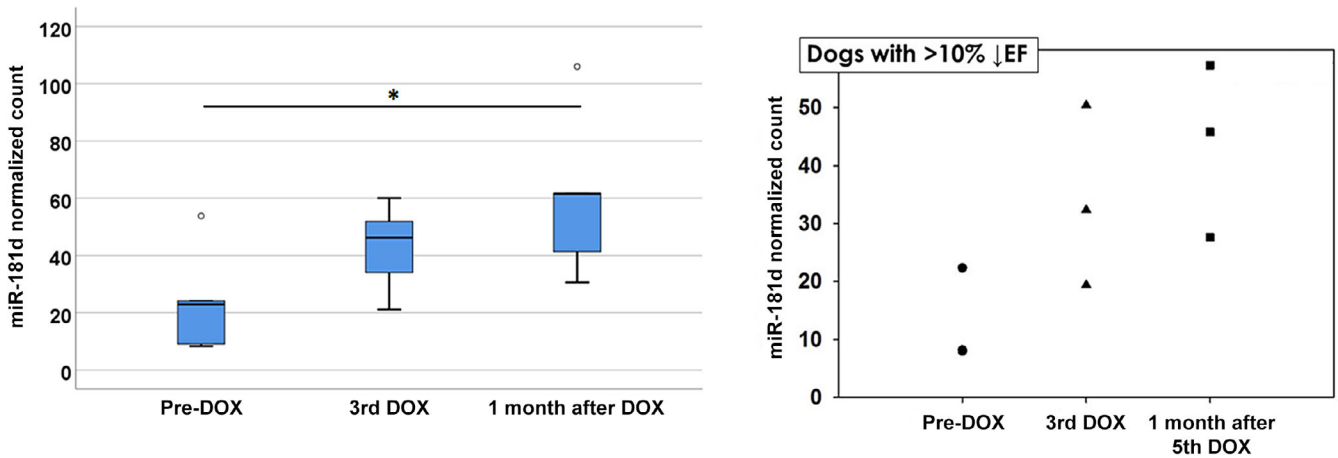


Figure 5 Box plot representing miR-181d level for all dogs with decreased LVEF (left, $n = 5$) and those with greater than 10% decrease in LVEF (right, $n = 3$) secondary to DOX treatment. Linear mixed model analysis showed significant upregulation over time ($P = .01$) for all dogs with decreased LVEF and also for dogs with greater than 10% decrease in LVEF ($P = .02$). Pairwise comparison also showed significant increase in miR-181d when comparing pre-DOX to post-DOX dogs ($P = .32$). Large asterisk denotes statistical significance. Open circles denote outliers

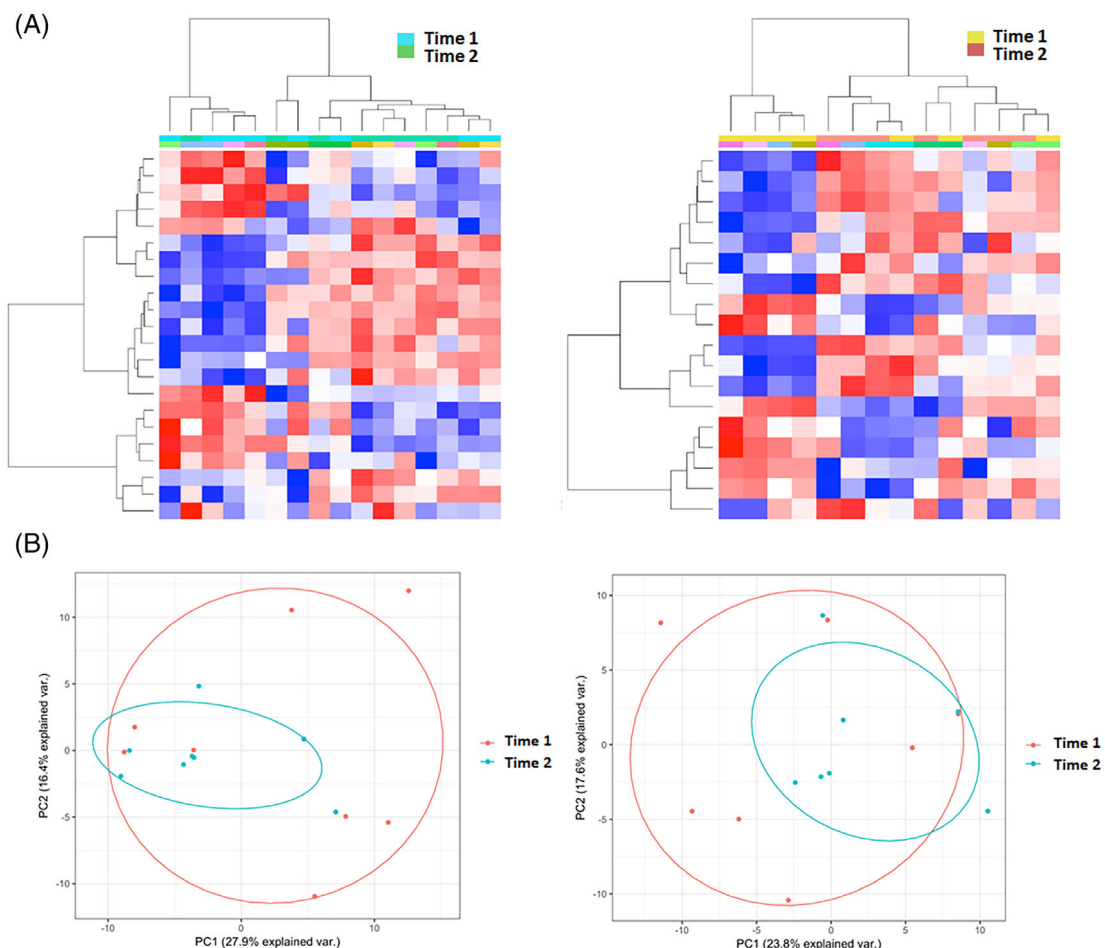


Figure 6 Hierarchical cluster analysis (A) and principal component analysis (B) of miRNA levels as a function of treatment time points. Hierarchical cluster analysis showed greater separation of miRNA profiles between post-DOX (time 3) and pre-DOX (time 1) than between during DOX (time 2) and pre-DOX (time 1). Principal component analysis showed that DOX treatment led to clustering of the miRNA profiles at both subsequent time points ($n = 8$)

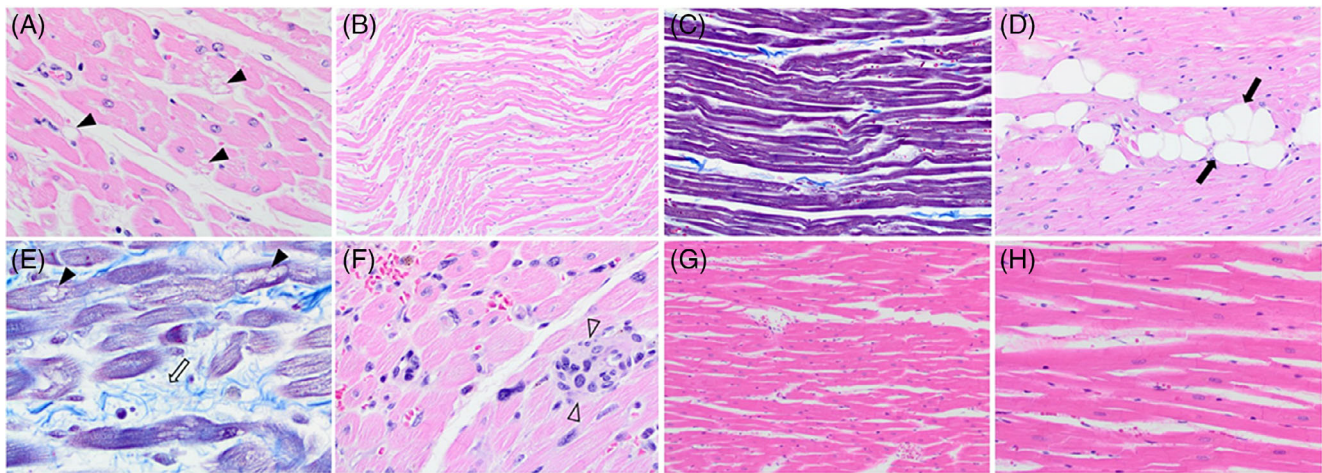


Figure 7 Cardiac histopathology from DOX-treated dogs shows lesions with characteristics of doxorubicin toxicity. A, Ventricular cardiomyocyte vacuolation (closed arrowheads) (hematoxylin and eosin), B, atrophic cardiomyocytes [hematoxylin and eosin], C, (phosphotungstic acid-hematoxylin), D, cardiomyocyte loss with fatty change (between closed arrows) (hematoxylin and eosin), E, atrial interstitial fibrosis (open arrow) and cardiomyocyte vacuolation (closed arrowheads) (Trichrome), F, cellular disorganization, hypertrophic and hyperplastic arteriolar wall (between open arrowheads) (hematoxylin and eosin), G, H, normal cardiomyocytes shown for comparison (hematoxylin and eosin)

pre-DOX ($P = .037$; fold-change, -3.1), as was miR-146a post-DOX compared to pre-DOX ($P = .013$; fold-change, -1.8). On the other hand, miR-502 was significantly upregulated both during DOX ($P = .01$; fold-change, 1.7) and post-DOX ($P = .003$; fold-change, 2) compared to pre-DOX. When stratifying miRNA expression based on change in LVEF, significant upregulation of miR-181d was noted post-DOX compared to pre-DOX in the group of dogs with decreased LVEF ($n = 5$, $P = .01$) and specifically those with $>10\%$ decrease in LVEF ($n = 3$; $P = .02$; Figure 5). In addition, a negative correlation was found between the expression levels of miR-146a and miR-502 (-0.59 ; $P = .003$), as well as miR-146a and miR-181d (-0.50 ; $P = .02$), and a positive correlation was found between miR-181d and miR-502 (0.43 ; $P = .04$).

Hierarchical cluster analysis showed that the miRNA expression profiles at time 1 and time 2 were interspersed with each other. However, clearer separation between the profiles was seen at time 3 (Figure 6A). Principal component analysis also showed that the miRNA profiles varied more among dogs at time 1, but DOX treatment led to clustering of the miRNA profiles at both subsequent time points (Figure 6B).

3.7 | Restaging

Of the 8 dogs diagnosed with hemangiosarcoma, 7 were restaged during the treatment period. Metastasis was detected in only 1 dog that developed liver nodules. However, further diagnostic testing for these liver nodules was not performed.

3.8 | Histopathology

The hearts of 8 dogs were available for histopathologic review. All dogs were euthanized within 3 months post-DOX. Of those 8 dogs, 6

were euthanized <1 month after their last cardiac evaluation and the final plasma collection for EV-miRNA and cTnI analysis. Seven dogs had changes characteristic for DOX cardiotoxicity including ventricular cardiomyocyte vacuolation, atrophy of cardiomyocytes, cardiomyocyte loss with fatty change, atrial interstitial fibrosis, and cardiomyocyte vacuolation (Figure 7).

Based on previously published doxorubicin cardiotoxicity scoring criteria published previously,²⁶ 5 dogs had grade 1, 2 dogs had grade 2, and 1 dog had no sign of cardiotoxicity on histology. All changes were noted in the right ventricle except for 1 of the grade 1 dogs with changes in the left ventricle that contained areas of infarction. One of the dogs with grade 2 toxicity also was the 1 with the largest increase in serum cTnI concentration and a decrease in LVEF $>10\%$. However, no significant correlations between histology grade and LVEF, cTnI, or miRNAs were found.

4 | DISCUSSION

In our study of canine cancer patients receiving single agent DOX chemotherapy, selected EV-miRNA were differentially expressed with DOX treatment: miR-107 and miR-146a were downregulated whereas miR-502 was upregulated after just 2 doses of DOX. Our results are similar to those seen in human pediatric patients receiving single agent anthracycline treatment that showed downregulation of total serum miR-107 1 year after completion of treatment, and downregulation of miR-146a 24 to 48 hours after the initiating of DOX treatment.¹⁷ Unlike the study of children, we did not find a correlation between these 2 miRNAs and LVEF, but our study utilized a much smaller sample size and may not have had sufficient statistical power to detect a correlation. The functional causes or consequences of miR-107 or miR-146a downregulation, or miR-502 upregulation in cardiomyocytes have not yet been fully elucidated. There are

conflicting reports regarding the protective and negative effects of miR-146a in the heart.^{27,28} The veterinary literature with regard to the role of miR-146a is sparse. Results in studies of humans supported the role of miRNA-146a in protection against inflammation, oxidative stress, apoptosis, or angiogenesis in atherosclerotic plaques.²⁹ Although miR-146a concentrations were increased in human patients with coronary artery disease,³⁰ they were found to inhibit matrix metalloproteinase-9 expression in human cardiomyocytes, suggesting a protective function against cardiac remodeling and myocardial dysfunction.²⁸ In rodent models, inhibition of miR-146a resulted in an increase in cardiac inflammation associated with diabetes.³¹ These findings suggest that the miR-146a downregulation found in the dogs treated with DOX in our study may be detrimental to cardiac function.

Similarly, miR-107 may have cardioprotective effects. Knockdown of miR-107 in mice has been shown to have detrimental effects, including decreases in cardiac function, cardiomyocyte size, and mitochondrial oxidative capacity.³² In addition, miR-107 is overexpressed in several tumor types such as colon, pancreas, and stomach cancers.³³⁻³⁵ Recent studies showed that breast cancer patients with higher miR-107 concentrations have significantly lower probability of metastasis-free survival.^{36,37} On the other hand, miR-502 has been shown to inhibit tumor cell proliferation in hepatocellular carcinoma in humans.³⁸

Based on our study, we cannot determine the source of change for miR-107, miR-146a, or miR-502. These changes may be associated with DOX-induced cardiotoxicity or with changes in the status of neoplasia (eg, change in tumor size, state of metastasis). However, re-staging of the tumor was performed for 7 of the 8 dogs used in the EV-miRNA analysis, and only 1 of the dogs developed new tumor sites (liver) during the course of the study. Studies thus far have only implicated the association of changes in miRNA-214 and miRNA-126 in plasma³⁹ and microvesicles with hemangiosarcoma in dogs.⁴⁰ Furthermore, tissue miRNA profiles of splenic hemangiosarcoma, splenic nodular hyperplasia, and normal spleen in dogs were found to differ.⁴¹ However, miR-107, miR-181d, miR-146a, and miR-502 were not noted to vary among these 3 tissue types. Results of these studies suggest that the miRNAs found to vary in our study did not originate from the tumor.

To better correlate miRNA changes with cardiac function, and therefore the status of cardiotoxicity, we further analyzed the miRNA profiles only of dogs with a decrease in LVEF, especially those with a >10% decrease in LVEF after completing DOX treatment. Within this particular group of dogs, miR-181d was significantly upregulated. The miR-181 family consists of 4 different miRNA species: miR-181a, miR-181b, miR-181c, and miR-181d. The genetic locations of miR-181a and miR-181b are closely clustered together, as are miR-181c and miR-181d in humans, dogs, and mice. All members of the miR-181 family have been shown to promote cell apoptosis by targeting proteins within the Bcl-2 family that regulates the cell autophagy and apoptosis balance.⁴²⁻⁴⁴ In addition, miR-181d targets leukemia inhibitory factor (LIF), which has been shown to enhance cardiac repair in rodent models after myocardial infarction.^{45,46} Therefore, an increase

in miR-181d would inhibit LIF and its cardioprotective effects. Increased miR-181d expression also may lead to an increased number of reactive oxygen species produced by mitochondria.⁴⁷ To confirm the exact source of the miRNA change in our patients, tissue (heart and tumor) miRNA would need to be analyzed concurrently. Nevertheless, miR-107, miR-146a, miR-181d, miR-502, or their combination showed potential as biomarkers for DOX-induced cardiotoxicity.

Our study showed increases in cTnI with DOX treatment but these increases were not significant until 1 month after completion of DOX treatment (post-DOX), and cTnI did not correlate with LVEF until 1 month after treatment completion. Another study found that cTnI concentrations as measured by ELISA increased with cumulative DOX doses, and a significant change was noted as early as week 3 of their chemotherapeutic protocol, a protocol that was similar to that used in our study.¹² In another study, significant increases in cTnI were found at the last treatment visit using a standard chemotherapeutic protocol similar to ours.¹⁰ However, these investigators did not have data available for comparison before the last visit. Interestingly, the highest cTnI concentrations recorded in the previous study for most of the dogs were 3 months after the end of treatment, indicating ongoing damage to the cardiomyocytes despite termination of treatment,¹⁰ a phenomenon also noted in our study. Given that cTnI is a marker of cardiac tissue damage, it is not surprising that cTnI would increase significantly with DOX treatment, but when cTnI is expected to increase and how it correlates to irreversible cardiac damage still is unknown. It is also unclear if an increase beyond a specific concentration could predict future cardiac dysfunction.

In human medicine, troponin has been used to predict risk of future cardiac complications rather than for early warning of irreversible cardiotoxicity. A systematic review showed that an early increase in troponin predicted the degree and severity of future left ventricular dysfunction.¹³ Patients with concentrations persistently higher than baseline, 1 month after completing chemotherapy had an 85% probability of major cardiac events within the 1st year of follow-up. A persistent negative troponin test, or no increase in troponin concentration, can identify, with a predictive negative value of 99%, patients with the lowest cardiotoxicity risk who will most likely never encounter cardiac complications and thus do not require intensive cardiac monitoring.¹³

Our study showed that LVEF as well as FS and FAC, 3 echocardiographic parameters of systolic function, decreased with increased cumulative DOX dose. We also found progressive cardiac enlargement (increase in LVIDd) with cumulative DOX treatment. Changes in LVIDd and FS may indicate development of cardiomyopathy, with systolic dysfunction. Indeed, a recent study in dogs showed that a decrease in FS with DOX treatment was associated with the development of cardiac clinical signs.⁴⁸ The relationship between cardiac injury and these echocardiographic parameters is further confirmed by the correlations between LVEF and FS with increasing concentrations of cTnI. However, the utility of these echocardiographic parameters for early cardiotoxicity detection cannot be confirmed in our study given the lack of significant changes between time points,

despite significant overall changes at the end of the study. This lack of statistical significance may be partly influenced by a decrease in sample size when performing Kruskal-Wallis analysis for time point comparisons versus linear mixed model analysis that considered overall change across all time points.

Histologic analysis indicated that 7 of the 8 (87.5%) dogs, the hearts of which were available for review had signs of cardiotoxicity, in contrast with the echocardiographic findings of only 6 of the 9 dogs (66.7%) having decreased LVEF. No significant correlation was found between histologic grades and cTnI or change in LVEF during DOX treatment, nor were any correlations observed between histologic grades and EV-miRNA expression levels. However, the samples for histology were collected later (at euthanasia), and therefore a direct comparison might not be valid. Nevertheless, using the LVEF criteria established in human cancer patients, only 1 of our study dogs would have been recommended for treatment termination. Therefore, our histopathologic findings suggest that echocardiographic measurements taken during the treatment period are not sensitive in predicting long-term DOX-induced cardiac injury.

Our study had some limitations. First, our sample size was small, and our results warrant further validation of EV-associated miR-107, miR-146a, miR-181d, and miR-502 as biomarkers for detecting DOX-associated cardiotoxicity at earlier stages. Also, miRNA profiles were not analyzed before each DOX administration and future studies should include analysis at each DOX treatment time point to better capture the exact timing of EV-miRNA change. In addition, histopathology samples were not collected at the same time as echocardiographic measurements and samples for cTnI and EV-miRNA evaluation, which might explain the lack of correlation between histopathology grading and the other measurements. If biopsy samples can be taken when the other variables are assessed, it then would be possible to correlate the echocardiographic, cTnI, and EV-miRNA expression changes with histologic signs of cardiotoxicity. However, given the invasive nature of biopsy, this was not feasible in our study. Also, histology findings consistent with cardiotoxicity were seen mostly within the right ventricle, which was not extensively studied by echocardiography. Further study should include echocardiographic evaluation of the right heart as well.

Furthermore, the miRNA results were analyzed using 2 different tests, DESeq2 and linear mixed model analysis, which likely created a more stringent list of miRNA candidates. Because of the limited number of miRNAs that reached statistical significance with the 2 analysis method, the false discovery rate criteria were not applied. Future validation studies with larger sample sizes may identify additional candidates that were missed in our study. An untreated control group also was not available for comparison.

In our study, point-of-care cTnI measurements were used and analysis of high-sensitivity cTnI tests could be considered in future studies. High-sensitivity cTnI test might have permitted detection of statistically significant changes earlier than the point-of-care cTnI testing. Finally, echocardiography was performed by 3 different echocardiographers, which might have introduced interobserver variability.

5 | CONCLUSION

We identified 4 miRNAs that were differentially expressed after administration of DOX: miR-107, miR-146a, miR-181d, and miR-502. Upregulation of miR-502 was detected before any significant changes were seen in other established biomarkers, including cTnI and echocardiographic parameters. In addition, miR-181d upregulation was noted in patients with a decrease in LVEF. Further study using a larger sample size is needed to validate our results. Nevertheless, our results show that EV-mRNAs are promising biomarkers for cardiotoxicity detection and may help clinicians modify treatment or implement cardioprotective strategies early to minimize irreversible cardiac damage.

ACKNOWLEDGMENTS

The authors acknowledge Dr. Bruce Barton for his assistance with statistical analysis. S. D. is supported by NIH grant RO1 HL122547 and AHA SFRN. Additional funding was provided by the Tufts University Companion Health Fund and Barkley Fund and Shipley Foundation.

CONFLICT OF INTEREST DECLARATION

Authors declare no conflict of interest.

OFF-LABEL ANTIMICROBIAL DECLARATION

Authors declare no off-label use of antimicrobials.

INSTITUTIONAL ANIMAL CARE AND USE COMMITTEE (IACUC) OR OTHER APPROVAL DECLARATION

Approved by the Tufts Cummings IACUC.

HUMAN ETHICS APPROVAL DECLARATION

Authors declare human ethics approval was not needed for this study.

ORCID

John E. Rush  <https://orcid.org/0000-0002-8277-8996>

Vicky K. Yang  <https://orcid.org/0000-0002-1281-4250>

REFERENCES

- Susanek SJ. Doxorubicin therapy in the dog. *J Am Vet Med Assoc.* 1983;182:70-72.
- Cappetta D, Rossi F, Piegari E, et al. Doxorubicin targets multiple players: a new view of an old problem. *Pharmacol Res.* 2018;127:4-14.
- Curigliano G, Mayer EL, Burstein HJ, Winer EP, Goldhirsch A. Cardiac toxicity from systemic cancer therapy: a comprehensive review. *Prog Cardiovasc Dis.* 2010;53:94-104.
- Cardinale D, Sandri MT. Detection and monitoring of cardiotoxicity by using biomarkers: pros and cons remarks on the international colloquium on cardioncology. *Prog Pediatr Cardiol.* 2015;39:77-84.
- Saeed MF, Premecz S, Goyal V, Singal PK, Jassal DS. Catching broken hearts: pre-clinical detection of doxorubicin and trastuzumab mediated cardiac dysfunction in the breast cancer setting. *Can J Physiol Pharmacol.* 2014;92:546-550.
- Bertinchant JP, Polge A, Juan JM, et al. Evaluation of cardiac troponin I and T levels as markers of myocardial damage in doxorubicin-induced cardiomyopathy rats, and their relationship with echocardiographic and histological findings. *Clin Chim Acta.* 2003;329:39-51.

7. DeFrancesco TC, Atkins CE, Keene BW, et al. Prospective clinical evaluation of serum cardiac troponin T in dogs admitted to a veterinary teaching hospital. *J Vet Intern Med.* 2002;16:553-557.
8. Mavinkurve-Groothuis AM, Kapusta L, Nir A, et al. The role of biomarkers in the early detection of anthracycline-induced cardiotoxicity in children: a review of the literature. *Pediatr Hematol Oncol.* 2008;25:655-664.
9. Todorova VK, Makhoul I, Wei J, Klimberg VS. Circulating miRNA profiles of doxorubicin-induced cardiotoxicity in breast cancer patients. *Ann Clin Lab Sci.* 2017;47:115-119.
10. Gallay-Lepoutre J, Belanger MC, Nadeau ME. Prospective evaluation of Doppler echocardiography, tissue Doppler imaging and biomarkers measurement for the detection of doxorubicin-induced cardiotoxicity in dogs: a pilot study. *Res Vet Sci.* 2016;105:153-159.
11. Selting KA, Lana SE, Ogilvie GK, et al. Cardiac troponin I in canine patients with lymphoma and osteosarcoma receiving doxorubicin: comparison with clinical heart disease in a retrospective analysis. *Vet Comp Oncol.* 2004;2:142-156.
12. Surachetpong SD, Teewasutrakul P, Rungsipipat A. Serial measurements of cardiac troponin I (cTnI) in dogs treated with doxorubicin. *Jpn J Vet Res.* 2016;64:221-233.
13. Dolci A, Dominici R, Cardinale D, Sandri MT, Panteghini M. Biochemical markers for prediction of chemotherapy-induced cardiotoxicity: systematic review of the literature and recommendations for use. *Am J Clin Pathol.* 2008;130:688-695.
14. Bartel DP. MicroRNAs: genomics, biogenesis, mechanism, and function. *Cell.* 2004;116:281-297.
15. Das S, Extracellular RNACC, Ansel KM, et al. The extracellular RNA communication consortium: establishing foundational knowledge and technologies for extracellular RNA research. *Cell.* 2019;177:231-242.
16. Holmgren G, Synnergren J, Andersson CX, Lindahl A, Sartipy P. MicroRNAs as potential biomarkers for doxorubicin-induced cardiotoxicity. *Toxicol in vitro.* 2016;34:26-34.
17. Oatmen KE, Toro-Salazar OH, Hauser K, et al. Identification of a novel microRNA profile in pediatric patients with cancer treated with anthracycline chemotherapy. *Am J Physiol Heart Circ Physiol.* 2018;315:H1443-H1452.
18. Ke X, Yang D, Liang J, et al. Human endothelial progenitor cell-derived exosomes increase proliferation and angiogenesis in cardiac fibroblasts by promoting the mesenchymal-endothelial transition and reducing high mobility group box 1 protein B1 expression. *DNA Cell Biol.* 2017;36:1018-1028.
19. Povero D, Panera N, Eguchi A, et al. Lipid-induced hepatocyte-derived extracellular vesicles regulate hepatic stellate cell via microRNAs targeting PPAR-gamma. *Cell Mol Gastroenterol Hepatol.* 2015;1:646-663. e644.
20. Corrado C, Raimondo S, Chiesi A, Ciccia F, de Leo G, Alessandro R. Exosomes as intercellular signaling organelles involved in health and disease: basic science and clinical applications. *Int J Mol Sci.* 2013;14:5338-5366.
21. van Eijndhoven MA, Zijlstra JM, Groenewegen NJ, et al. Plasma vesicle miRNAs for therapy response monitoring in Hodgkin lymphoma patients. *JCI Insight.* 2016;1:e89631.
22. Cornell CC, Kittleson MD, Della Torre P, et al. Allometric scaling of M-mode cardiac measurements in normal adult dogs. *J Vet Intern Med.* 2004;18:311-321.
23. Kozomara A, Birgaoanu M, Griffiths-Jones S. miRBase: from microRNA sequences to function. *Nucleic Acids Res.* 2019;47:D155-D162.
24. Love MI, Huber W, Anders S. Moderated estimation of fold change and dispersion for RNA-seq data with DESeq2. *Genome Biol.* 2014;15:550.
25. Thery C, Witwer KW, Aikawa E, et al. Minimal information for studies of extracellular vesicles 2018 (MISEV2018): a position statement of the International Society for Extracellular Vesicles and update of the MISEV2014 guidelines. *J Extracell Vesicles.* 2018;7:1535750.
26. Working PK, Newman MS, Sullivan T, Yarrington J. Reduction of the cardiotoxicity of doxorubicin in rabbits and dogs by encapsulation in long-circulating, pegylated liposomes. *J Pharmacol Exp Ther.* 1999;289:1128-1133.
27. Oh JG, Watanabe S, Lee A, et al. miR-146a suppresses SUMO1 expression and induces cardiac dysfunction in maladaptive hypertrophy. *Circ Res.* 2018;123:673-685.
28. Palomer X, Capdevila-Busquets E, Botteri G, et al. miR-146a targets Fos expression in human cardiac cells. *Dis Model Mech.* 2015;8:1081-1091.
29. Esplugas R, Arenas M, Serra N, et al. Effect of radiotherapy on the expression of cardiovascular disease-related miRNA-146a, -155, -221 and -222 in blood of women with breast cancer. *PLoS One.* 2019;14:e0217443.
30. Takahashi Y, Satoh M, Minami Y, Tabuchi T, Itoh T, Nakamura M. Expression of miR-146a/b is associated with the toll-like receptor 4 signal in coronary artery disease: effect of renin-angiotensin system blockade and statins on miRNA-146a/b and toll-like receptor 4 levels. *Clin Sci (Lond).* 2010;119:395-405.
31. Feng B, Chen S, Gordon AD, Chakrabarti S. miR-146a mediates inflammatory changes and fibrosis in the heart in diabetes. *J Mol Cell Cardiol.* 2017;105:70-76.
32. Rech M, Kuhn AR, Lumens J, et al. AntagomiR-103 and -107 treatment affects cardiac function and metabolism. *Mol Ther Nucleic Acids.* 2019;14:424-437.
33. Ayremloou N, Mozdarani H, Mowla SJ, Delavari A. Increased levels of serum and tissue miR-107 in human gastric cancer: correlation with tumor hypoxia. *Cancer Biomark.* 2015;15:851-860.
34. Liu F, Liu S, Ai F, et al. miR-107 promotes proliferation and inhibits apoptosis of colon cancer cells by targeting prostate apoptosis response-4 (Par4). *Oncol Res.* 2017;25:967-974.
35. Xiong J, Wang D, Wei A, et al. Deregulated expression of miR-107 inhibits metastasis of PDAC through inhibition PI3K/Akt signaling via caveolin-1 and PTEN. *Exp Cell Res.* 2017;361:316-323.
36. Martello G, Rosato A, Ferrari F, et al. A MicroRNA targeting dicer for metastasis control. *Cell.* 2010;141:1195-1207.
37. Volinia S, Calin GA, Liu CG, et al. A microRNA expression signature of human solid tumors defines cancer gene targets. *Proc Natl Acad Sci U S A.* 2006;103:2257-2261.
38. Chen S, Li F, Chai H, Tao X, Wang H, Ji A. miR-502 inhibits cell proliferation and tumor growth in hepatocellular carcinoma through suppressing phosphoinositide 3-kinase catalytic subunit gamma. *Biochem Biophys Res Commun.* 2015;464:500-505.
39. Heishima K, Ichikawa Y, Yoshida K, et al. Circulating microRNA-214 and -126 as potential biomarkers for canine neoplastic disease. *Sci Rep.* 2017;7:2301.
40. Heishima K, Mori T, Ichikawa Y, et al. MicroRNA-214 and microRNA-126 are potential biomarkers for malignant endothelial proliferative diseases. *Int J Mol Sci.* 2015;16:25377-25391.
41. Grimes JA, Prasad N, Levy S, et al. A comparison of microRNA expression profiles from splenic hemangiosarcoma, splenic nodular hyperplasia, and normal spleens of dogs. *BMC Vet Res.* 2016;12:272.
42. Ouyang YB, Lu Y, Yue S, Giffard RG. miR-181 targets multiple Bcl-2 family members and influences apoptosis and mitochondrial function in astrocytes. *Mitochondrion.* 2012;12:213-219.
43. Qian YQ, Jiang JN, Peng J, Wang Q, Shen Y. Evaluation of MiR-181a as a potential therapeutic target in osteoarthritis. *Trop J Pharm Res.* 2017;16:1069-1075.
44. Wu XF, Zhou ZH, Zou J. MicroRNA-181 inhibits proliferation and promotes apoptosis of chondrocytes in osteoarthritis by targeting PTEN. *Biochem Cell Biol.* 2017;95:437-444.

45. Berry MF, Pirollo TJ, Jayasankar V, et al. Targeted overexpression of leukemia inhibitory factor to preserve myocardium in a rat model of postinfarction heart failure. *J Thorac Cardiovasc Surg.* 2004;128:866-875.
46. Kanda M, Nagai T, Takahashi T, et al. Leukemia inhibitory factor enhances endogenous cardiomyocyte regeneration after myocardial infarction. *PLoS One.* 2016;11:e0156562.
47. Das S, Kohr M, Dunkerly-Eyring B, et al. Divergent effects of miR-181 family members on myocardial function through protective cytosolic and detrimental mitochondrial microRNA targets. *J Am Heart Assoc.* 2017;6.
48. Hallman BE, Hauck ML, Williams LE, Hess PR, Suter SE. Incidence and risk factors associated with development of clinical cardiotoxicity in dogs receiving doxorubicin. *J Vet Intern Med.* 2019;33:783-791.

SUPPORTING INFORMATION

Additional supporting information may be found online in the Supporting Information section at the end of this article.

How to cite this article: Beaumier A, SR Robinson, Robinson N, et al. Extracellular vesicular microRNAs as potential biomarker for early detection of doxorubicin-induced cardiotoxicity. *J Vet Intern Med.* 2020;34:1260-1271. <https://doi.org/10.1111/jvim.15762>